

Polyelectrolyte adsorption study on polyethersulfone membrane during polymer-enhanced ultrafiltration by electrochemical impedance spectroscopy

M. Palencia · B. L. Rivas · E. Pereira · A. Arrieta

Received: 20 August 2009 / Revised: 30 November 2009 / Accepted: 20 December 2009 /
Published online: 8 January 2010
© Springer-Verlag 2010

Abstract Electrochemical impedance spectroscopy (EIS) was used to study the fouling produced due to the adsorption of poly(vinyl sulfonic acid) on polyethersulfone membrane during metal ion recovery by polymer-enhanced ultrafiltration (PEUF). A solution of PVSA (40 mM in monomeric unit and pH 3.0, 4.5, and 6.0) was placed in a ultrafiltration cell, and then a stream of metal ions (2.0 mM in Co^{2+} , Ni^{2+} , Cu^{2+} , Zn^{2+} , Cd^{2+} , and Pb^{2+}) was passed from reservoir to cell. Fouled membranes were studied by EIS at low and intermediate frequencies. Measurements of hydrodynamic permeability and ATR-FTIR spectra were also obtained. Different relaxation processes were observed with characteristic frequencies (f_0) ~ 78 kHz and $f_0 \sim 3562$ kHz for active layer and clean membrane, respectively, while the frequencies for the fouled membrane $f_0 = \sim 79.4$ and $f_0 = \sim 2511.9$ kHz (pH 3.0). The value of f_0 could not be defined at pH 6.0. The relaxation times obtained were in the order of $\times 10^{-5}$ and $\times 10^{-3}$ s approximately for all cases. Our results suggest that relaxation mechanisms, at intermediate frequencies, can mainly be associated to polarization processes or to the migration of charge carriers.

Keywords Electrochemical impedance spectroscopy · Polymer enhanced ultrafiltration · Fouling · Polyelectrolyte · Equivalent circuit

M. Palencia · B. L. Rivas (✉)

Department of Polymer, Faculty of Chemistry, University of Concepción, Casilla 160-C,
Concepción, Chile
e-mail: brivas@udec.cl

E. Pereira

Department of Analytic and Inorganic Chemistry, University of Concepción, Casilla 160-C,
Concepción, Chile

A. Arrieta

Group of Development and Application of New Materials, Pontificia Bolivariana University,
Montería, Colombia

Introduction

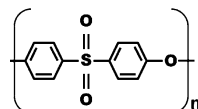
Membrane technology has been found to be an attractive alternative for the separation of different substances in a large variety of processes. Additionally, it is faster, energy efficient, and does not involve any phase change [1]. At present, the application of ultrafiltration in membrane technology is growing very rapidly in the pharmaceutical, chemical, paper, semiconductor, and dairy industries. Metal ion recovery can be achieved efficiently by combining a water-soluble polymer (WSP) with ultrafiltration processes, and this technique is commonly referred to polymer-enhanced ultrafiltration (PEUF) or liquid-phase polymer-based retention (LPR) [2, 3].

An appreciable number of WSP with sulfonic groups was previously used in metal ion recovery by PEUF [2, 4] and extensively employed in ion-exchange resins [4]. In addition to WSP, another important component in PEUF is the ultrafiltration membrane because it partially determines process continuity. Furthermore, the pore size distribution (or pore density) and the thickness of the membrane's active layer are the main factors determining the flux and retention features, although these parameters are strongly influenced by the material's chemical composition, which has a great influence on adsorption and fouling mechanisms on the surface and inside the pores [1, 5]. In short, the main factors determining of the membrane behavior during filtration are the structure, the chemical composition, and the operation conditions [5]. For example, polyethersulfone (PES) is a kind of special polymer with good performances (such as excellent mechanical properties, good heat resistance, and stability at wide pH range). However, its hydrophobicity controlled due to the PES structure leads to low membrane flux and easy fouling, which greatly affect a separation membrane's application field and usage life.

The PES structure used in this article is shown in Fig. 1. Recently, researchers have synthesized several different kinds of hydrocarbon-based sulfonated polymers, like PES, for fuel cell membrane to overcome the problems of the perfluorosulfonated polymers [6].

On the other hand, impedance spectroscopy (IS) appears to play an important role in the fundamental and applied electrochemistry and material science in the coming years. One of the most attractive aspects of IS is as a tool for investigating both electrical and electrochemical properties of materials and systems, these are often the direct connection that exists between real system behavior and that of an idealized model circuit consisting of discrete electrical components [7–12]. Therefore, impedance data are frequently compared with an equivalent circuit, which represent the physical processes taking place in the studied system [7, 11]. This technique has been used to predict aspects of the performance of chemical sensors and fuel cells, to investigate membrane behavior in living cells and in the

Fig. 1 Polyethersulfone structure (PES)



interpretation of fundamental electrochemical and electronic processes [12]. It was recently used in the synthetic polymer membrane in the study of ultrafiltration membrane properties [10, 13], the fouling of ion-exchange membranes [14] and reverse osmosis membranes [15] as well as to determine the electrical properties of the supported liquid membranes, such as, the electrical resistance and capacitance under working conditions in contact with saline solutions [16].

In this article, using IS, we analyze the electrochemical behavior and the features of the fouling produced as a result of adsorption of a polyelectrolyte on PES membrane during metal ion recovery by PEUF when poly(vinyl sulfonic acid) is used as WSP. Here, we show the measurements and fouling simulation obtained from IS experiments. Aspects related with polymer–metal ion interaction, membrane–metal ion interaction, and membrane–polymer interaction will be discussed in separate documents.

Experimental

Reagents

Poly(vinyl sulfonic acid), PVSA (solution 25%, Aldrich, Mw: 250000 Da, $d:1.267 \text{ kg L}^{-1}$, $n_D^{20}:1.3890$) was used as WSP. In the feed, different nitrates with a general expression $M^{n+}(\text{NO}_3) \cdot X\text{H}_2\text{O}$ were used (analytical grade from Merck). These included the ions Co^{2+} , Ni^{2+} , Cu^{2+} , Zn^{2+} , Cd^{2+} , and Pb^{2+} with X being: 6, 6, 2.5, 6, 4, and 0, respectively, constituting a single metal ion solution. For filtration experiments, PES disk-shaped membranes (Biomax PBGC; nominal cut-off of 10000 Da; $n_D^{20}:1.653$; 44.5 mm in diameter; manufactured by Amicon Bioseparations-Millipore Co.) were used in all the experiments.

Production of fouling on the membrane by adsorption of polyelectrolyte (filtration experiment)

The membranes were fouled during metal ion recovery by PEUF using the enrichment method. A description of the filtration system used for these measurements is shown in Fig. 2. In each PEUF experiment, a solution of 40 mM of polymer (in terms of the monomer with molar mass of 130 g mol^{-1}) at pH 3.0, 4.5, and 6.0 was placed inside a stirred ultrafiltration cell with a volume of 25 mL and an effective membrane area of 13.4 cm^2 . The feed was a 2.0-mM solution of metal ion nitrates (nitrates of Co^{2+} , Ni^{2+} , Cu^{2+} , Zn^{2+} , Cd^{2+} , Pb^{2+}) at the polymer solution's pH. The pH was adjusted by using HNO_3 and NaOH solutions. The system was operated at 300 kPa of pressure, using pressurized nitrogen, and at 200 rpm surface stirring rate. The membranes were previously hydrated for 24 h approximately. An experimental blank was performed before and after each PEUF experiment. These blank runs consisted in the filtration of the metal ion solution under the same experimental conditions but without polymer.

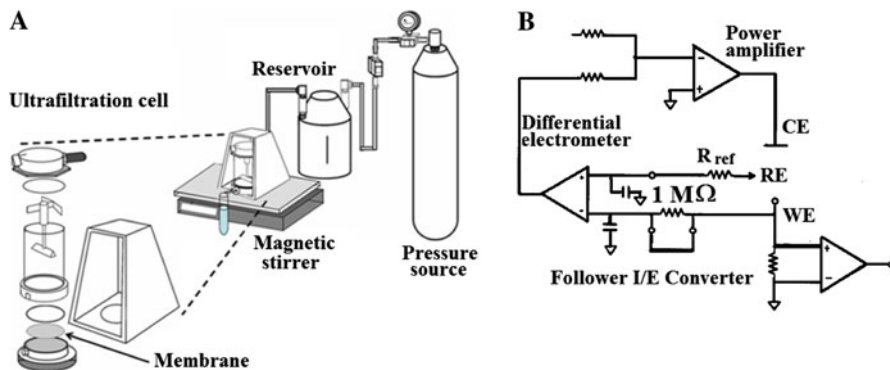


Fig. 2 a Components of ultrafiltration system and b simplified scheme of potentiostat (conventional three-electrode cell configuration)

Permeability measures

At the beginning and end of the filtration process, a *permeability test* was performed: the bi-distilled water mass permeated and the time of permeation was measured at the different applied pressures (from 150 to 350 kPa) maintaining a constant volume in the filtration cell. The mass was measured with a high precision balance with errors below $\pm 1 \times 10^{-7}$ kg (Sartorius Analytic A120S). A *bi-distilled water wash* was realized after each filtration step (experimental blank and LPR experiment): bi-distilled water was used for rinsing and then 50 mL of bi-distilled water was passed through filtration cell.

Electrochemical impedance spectroscopy

A small portion (1 cm \times 1 cm) of the membrane was analyzed in each case. Electrochemical impedance spectroscopy (EIS) measurements were performed at room temperature (25 °C) using a conventional three-electrode cell configuration (auxiliary electrode, reference electrode Ag/AgCl, and work electrode). The electrochemical cell was connected to a potentiostat (Parstat 2263 EG&G), which includes a galvanostat as well as hardware with interface to a PC (see Fig. 2b).

Impedance measurements were to carry out using the single-sine technique: a sequence of impedance measurements were made starting at an initial frequency (100 kHz) and stopping at a final frequency (0.1 Hz). The alternate current amplitude voltage used for the experiments was 10 mV. Prior to the impedance experiment, the potentiostat, analyzer, computer, and software functioning were verified by a dummy cell (Randle's cell), which simulates an electrochemical cell and consists in a 1-k Ω resistor (R_1) in series with a 10-k Ω resistor (R_2) in parallel with a 10-mF capacitor (C) (see Fig. 3a). The impedance spectra (from Nyquist and Bode plot) were further analyzed by using a simulation program of ZSimpWin V3.10. In a Nyquist plot, the imaginary component of impedance (Z'') is plotted versus the real component of impedance (Z') at each excitation frequency

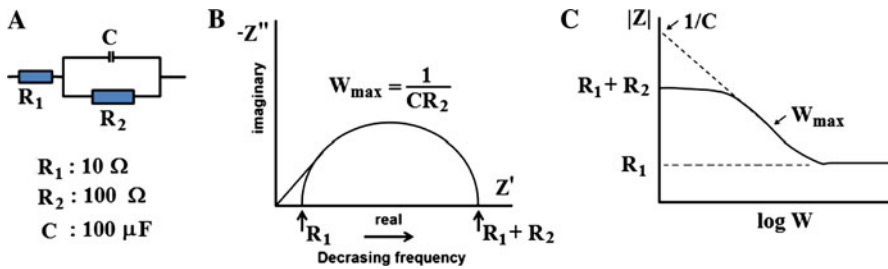


Fig. 3 Dummy cell of calibration: **a** equivalent circuit, **b** Nyquist diagram, and **c** Bode diagram

(see Fig. 3b); in a Bode plot, the absolute value of impedance ($|Z|$) is plotted versus the logarithmic of frequency (see Fig. 3c).

ATR-FTIR spectrum

ATR-FTIR spectroscopy using a Nicolet instrument equipped with DTGS-KBr detector (OMNIC 5.2a, Nicolet Instrument Corp.) was applied to analyze the surface chemistry of both clean and fouled membranes. A total of 64 scans were performed at a resolution of 4 cm^{-1} using a diamond crystal; the temperature and mirror velocity was $20 \text{ }^\circ\text{C}$ and 0.9494 , respectively.

Results and discussion

Permeability measurements

The hydrodynamic permeability for clean membrane (L_0) and for fouled membrane (L_f) at the pHs studied was determined from changes in the flux (J) due to changes of pressure (P). The values obtained for clean membrane were: L_0 (pH: 3.0): $9.3 \times 10^{-11} \text{ ms}^{-1} \text{ Pa}^{-1}$, L_0 (pH: 4.5): $2.7 \times 10^{-10} \text{ ms}^{-1} \text{ Pa}^{-1}$, and L_0 (pH: 6.0): $4.9 \times 10^{-10} \text{ ms}^{-1} \text{ Pa}^{-1}$, and the values obtained for fouled membranes were: L_f (pH: 3.0): $5.3 \times 10^{-11} \text{ ms}^{-1} \text{ Pa}^{-1}$, L_f (pH: 4.5): $6.5 \times 10^{-11} \text{ ms}^{-1} \text{ Pa}^{-1}$, and L_f (pH: 6.0): $8.7 \times 10^{-11} \text{ ms}^{-1} \text{ Pa}^{-1}$. Additionally, a significant effect on permeability was observed as a function of pH: it decreased as acidity increased with changes of ~ 43 , ~ 76 , and $\sim 82\%$ for fouled membranes with respect to clean membranes at pH 3.0, 4.5, and 6.0, respectively. The decrease in permeability is associated with the increase in membrane's resistance to passing water molecules, clearly indicating greater adsorption of PVSA (larger fouling) on the surface membrane with the decrease of pH during PEUF.

Impedance spectrum and equivalent circuit of clean membrane

In the case of clean membranes, three measured groups were considered since the PES membrane used corresponds to an asymmetric membrane, and therefore two parts are forming the membrane: polymeric support (polyolefin) and active layer

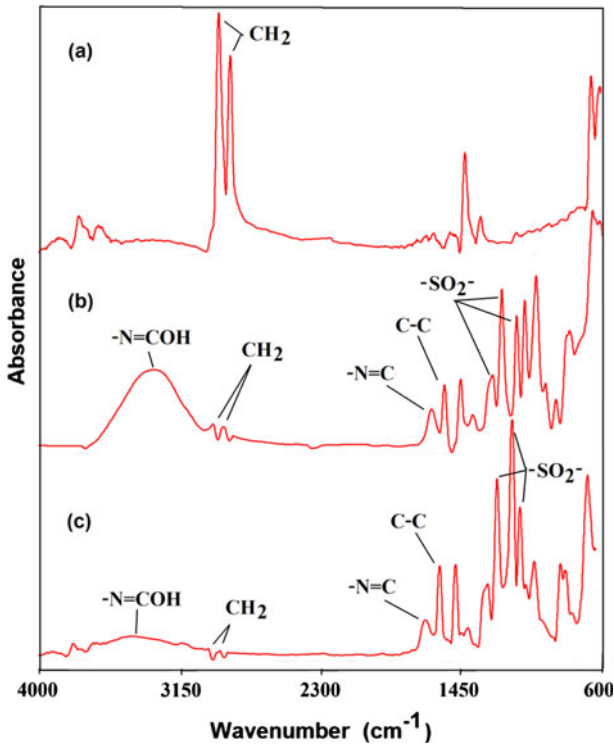


Fig. 4 ATR-FTIR spectrums: **a** support (polyolefin), **b** active layer (polyethersulfone), and **c** fouled membrane by adsorption of poly(vinyl sulfonic acid)

(PES). Structural differences and characteristic groups for each component can be observed from the respective ATR-FTIR spectra (see Fig. 4a, b); the principal signals are given in the Table 1.

For polymeric support, EIS spectrum was obtained only for frequencies from 100 to ~ 0.85 kHz, because the dispersion data between consecutive points were too great at high frequencies. This erratic behavior was the principal limitation for the spectra in all cases. For the support, the equivalent circuit was found to be a resistor in series with a CPE (constant phase element) (see Fig. 5a). The appearance of CPE as a component of circuit could be due to the varying thickness (roughness) and the support's composition. Other researchers have reported the appearance of CPE behavior at low frequencies for polymers derived from aryl amines and ring-substituted aryl amines [17]. Only one process of dielectric relaxation was observed in the Bode diagram with a characteristic frequency (f_0) around 78 kHz and a relaxation time (τ) of 0.002 s.

For the active layer, the IS spectrum was obtained for intermediate frequencies from 100 to ~ 1 kHz. The equivalent circuit was described by a Randles circuit, with $R_2 \gg R_1$ and a very low capacitance (with an order around multiplicative inverse of resistance according to simulation results). R_2 was found to be equal to $2.89 \times 10^6 \Omega \text{ cm}^2$, R_1 was negligible with respect to R_2 , and the capacitance was

Table 1 Main IR bands of different membrane components: *support* (polyolefin), *active layer* [polyethersulfone (PES) and polyvinylpyrrolidone (PVP) as additive], and *foulant* [poly(vinyl sulfonic acid) (PVSA)]

Wavenumber (cm ⁻¹)	Groups	Component of membrane (clean or fouled)
~2879	Tension symmetric -CH ₂ -	Support, additive (PVP) and foulant (PVSA)
~2940	Tension asymmetric -CH ₂ -	Support, additive (PVP) and foulant (PVSA)
~1660	Vibrations of -N=C	Additive (PVP)
~3360–3240	Vibrations of -N=C-OH	Additive (PVP)
~1580	Aromatic C-C bond	Active layer (PES)
~1150, ~1296, and ~1240	Sulfone group	Active layer (PES) and foulant (PVSA)

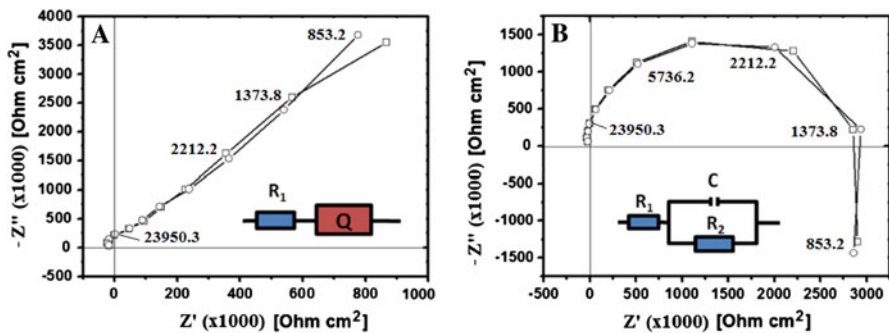


Fig. 5 Nyquist diagram and equivalent circuit for **a** support (polyolefin) and **b** active layer (polyethersulfone) from experimental data

around 1 μF/cm² (see Fig. 5b). Two processes of dielectric relaxation were observed from the Bode diagram at intermediate frequencies ($f_0 = \sim 3562$ kHz) and low frequencies ($f_0 = \sim 3.59$ kHz), where the dielectric relaxation process at intermediate frequencies is more clearly identified. The relaxation times were 4.46×10^{-5} and 0.044 s, respectively. Additionally, a negative capacitance was observed at lower frequency values between ~ 0.85 and ~ 0.20 kHz.

The real configuration during PEUF experiments for the clean membranes is active layer and polymeric support; the IS spectrum was obtained for frequencies from 100 to $\sim 1 \times 10^{-3}$ kHz. Not a single equivalent circuit was observed for the description of the obtained spectrum (see Fig. 6a, b, c); therefore, an adequate representation of experimental data for an exact description of physical model was not possible (in a physical model, each one of the model components must be considered to come from a physical process in the electrochemical system). Three resistances and two capacitors were necessary to define the equivalent circuits, but given that R_2 and $R_3 \gg R_1$, only two resistors (R_2 and R_3) were found to be significantly important, where $R_2 \approx 1 \times 10^6$ and $R_3 \approx 1.5 \times 10^6 \Omega \text{ cm}^2$ (see Fig. 6d, e).

Two processes of dielectric relaxation were observed from the Bode diagram at intermediate ($f_0 = \sim 3562$ kHz) and low frequencies ($f_0 = \sim 78.8$ kHz). Note that

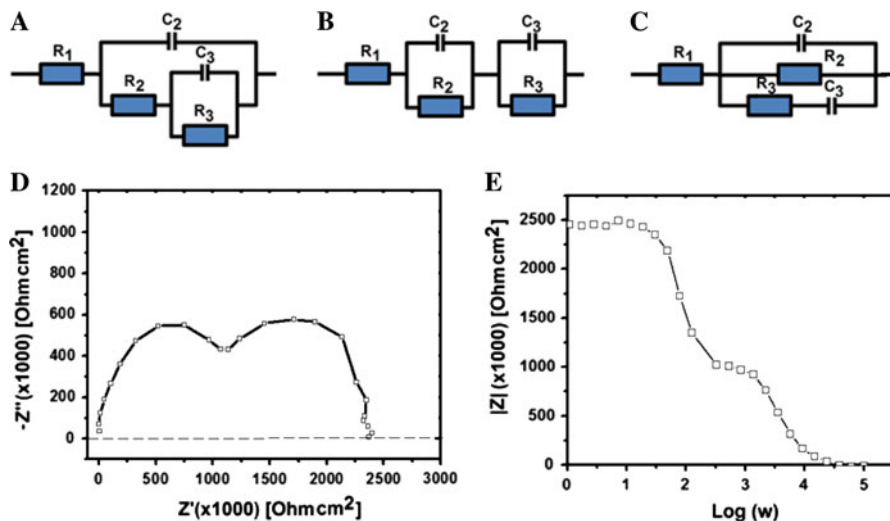


Fig. 6 Impedance spectra of virgin membrane of PES: **a**, **b**, and **c** possible equivalent circuits from modeling by software, **d** Nyquist diagram, and **e** Bode diagram from experimental data

these values correspond to those obtained for the active layer and polymeric support, respectively. Therefore, the PES membrane can be associated to two dielectric relaxation processes at intermediate and low frequencies related to each main component (support and active layer).

EIS for fouled membrane and equivalent circuit

After the filtration experiment, part of the PVSA inside the ultrafiltration cell during PEUF has been adsorbed on the membrane's surface as observed in the permeability data ("Permeability measurements" section) and from the changes in the adsorption bands in the ATR-FTIR spectrum (Fig. 4b, c). Given that the presence of any solvent or additives affects a polymer's morphology. Additionally, due to its dielectric properties, it is expected that fouled membrane shows a different dielectric behavior in comparison with the clean membrane.

Figure 7 presents the Nyquist and Bode diagrams at pH 3.0 and 6.0 for fouled membranes (PES/PVSA). From Nyquist plot, it can be seen that the impedance spectra for the fouled membrane were different at the different pH studied (see Fig. 7a, c). On the other hand, from the Bode diagrams, it was possible to see that the Nyquist diagram does not adequately represent the experimental data since the dispersion and erratic behavior of measures at higher frequencies was more significant (see Fig. 7b, d).

The value of R_2 , $\sim 5 \times 10^5 \Omega \text{ cm}^2$, for PES/PVSA at pH 3.0 decreases appreciably with respect to the clean and fouled membranes at pH 6.0, where the latter is around $\sim 2.25 \times 10^7 \Omega \text{ cm}^2$. The decreased resistance can be explained by a major adsorption of PVSA- M^{n+} on the PES surface during the PEUF experiments. Additionally, two relaxation processes were observed at pH 3.0 and

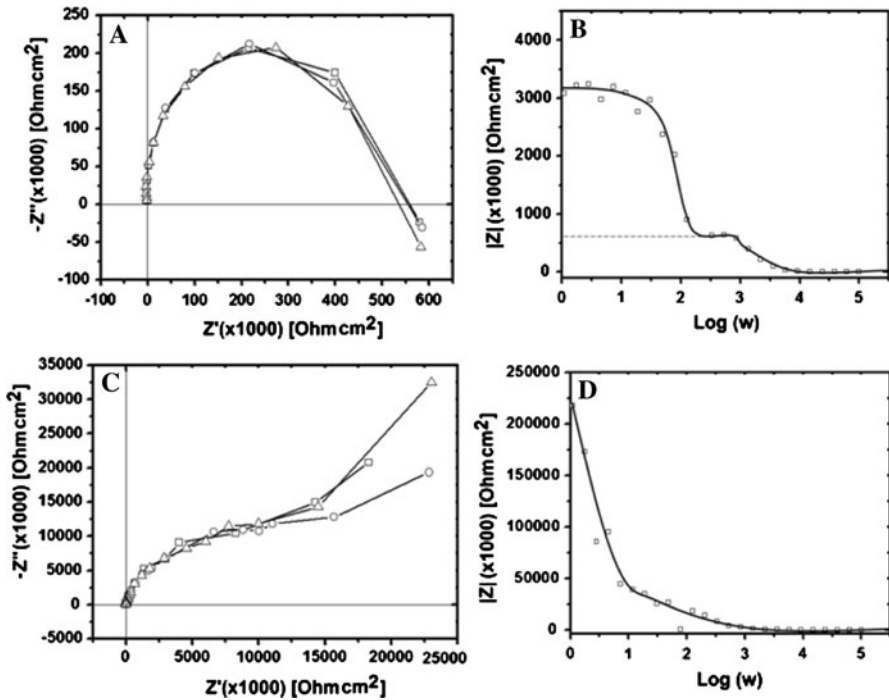


Fig. 7 Impedance spectra of membrane fouled with PES/PVSA from experimental data: **a, b** Nyquist and Bode diagrams at pH 3.0, respectively, and **c, d** Nyquist and Bode diagrams at pH 6.0, respectively

intermediate frequencies with characteristic frequency values of $f_0 = \sim 79.4$ kHz and $f_0 = \sim 2511.9$ kHz. At pH 6.0, a value of f_0 could not be defined.

pH dependence is directly related to the amount of PVSA adsorbed on the surface since the interaction membrane-WSP is strongly influenced by pH, and consequently the membrane’s dielectric properties are modified in each case. Generally, the dielectric parameter is expected to depend on the polymer concentration since the relationship between local chain conformation and polyion effective charge can depend on the concentration, flexibility and contour length of the adsorbed polyelectrolyte as well as its interactions with small ions (counterions and adsorbed metal ions). When PEUF is taking place, the PVSA in the inside cell corresponds to a polyelectrolyte in solution interacting with metal ions that are continually entering into the cell. In this case, two types of counterions are considered: “bound” counterions that are near the charged polymer and “free” counterions that are distant from the polymer chain, interacting through a screened coulomb potential. However, when the polymer has been absorbed and the sample is analyzed by IS, only the effect of “bound” counterions should be considered.

When an electric field is applied to an ultrafiltration membrane (clean or fouled), where this is a dielectric material, the resulting polarization can be divided in two parts according to the response’s time constant: an almost instantaneous polarization due to electron displacement with respect to the nuclei which is associated to a high-frequency dielectric constant and a time-dependent polarization due to the

Table 2 Component values for each equivalent circuit obtained for fouled membranes at pH 6.0

Component	Circuit No. 1	Circuit No. 2	Circuit No. 3
R_1 ($\Omega \text{ cm}^2$)	~ 0	~ 0	~ 0
R_2 ($\Omega \text{ cm}^2$)	1.95×10^7	3.2×10^7	6.0×10^7
R_3 ($\Omega \text{ cm}^2$)	2.5×10^7	1.6×10^7	3.0×10^7
C_2 ($\mu\text{F}/\text{cm}^2$)	1	1	1.5
C_3 ($\mu\text{F}/\text{cm}^2$)	10	0.1	6.0

Equivalent circuits 1, 2, and 3 correspond to circuits of Fig. 6a, b, and c, respectively

orientation of dipoles in the electric field (electronic polarization, atomic or ionic polarization, dipolar polarization, spontaneous polarization and interface, or space charge polarization) [18, 19]. Since the polarization due to the elastic displacement of electron clouds of the particles (atoms and molecules) requires very little time ($<10^{-12}$ s) [19], the relaxation times obtained, between 10^{-5} and 10^{-3} s approximately for all cases, suggest that the relaxation mechanisms at intermediate frequencies are probably associated to the polarization involving particle movement, such as the orientation of permanent dipoles or the migration of charge carriers (electrons or ions), which requires a much longer time to be performed [19].

On the one hand, at pH 3.0, the circuit equivalent to the impedance spectrum for the active layer was described by a Randles circuit (Fig. 5b). On the other hand, several equivalent circuits could be assigned to fouled membrane at pH 6.0, where these are similar to those obtained to describe a virgin membrane (Fig. 6a, b, c). Simulation results, presented in the Table 2, show that the relation between capacitors and resistance changes depends on the equivalent circuit, making it more difficult to assign a physical equivalent. Additionally, the R_1 obtained was negligible in comparison with R_2 , indicating that this element could be omitted from the circuit model due to PES's excellent dielectric properties.

At pH 4.5, different spectra were observed for a same sample (see Fig. 8) and these became repetitive after several measures (a total of 40 consecutive measurements in this case). These changes suggest that the components (resistors and capacitor) of the equivalent circuit in the system PES/PVSA should not be considered constants, but rather that depend on frequency.

Conclusions

Adsorption of PVSA on a PES membrane during PEUF produces changes in the dielectric response of fouled membrane in comparison with clean membrane at intermediate and low frequencies. In the case of the clean membrane, its different components present dielectric responses, which can be observed when these are analyzed on the whole, showing two dielectric relaxation processes. An active layer was described by Randles with $R_n \gg R_1 \approx 0$ ($n = 2$), where this observation is similar for all cases studied at different pH (3, 4.5, and 6) with $n = 2$ and 3. An adequate representation of experimental data for an exact description of the physical

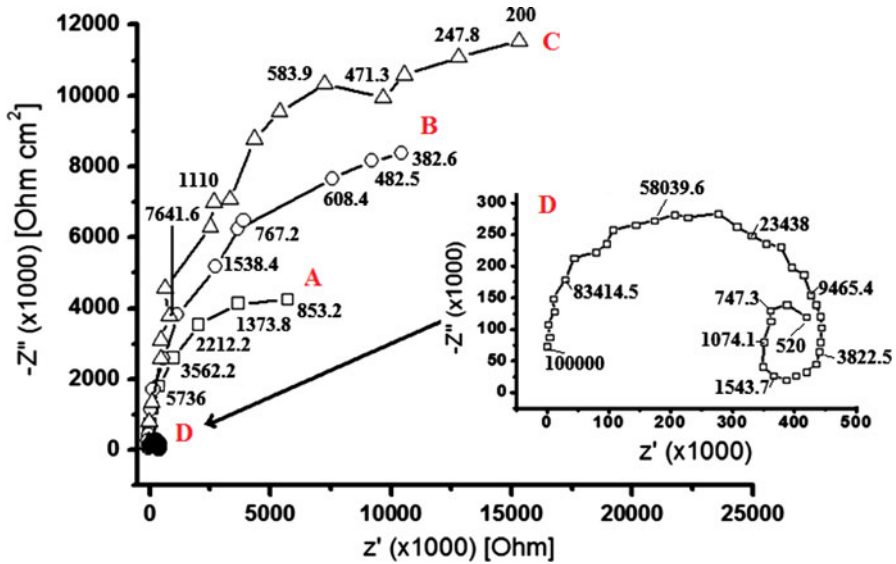


Fig. 8 Nyquist diagram of fouled membrane of PES/PVSA at pH 4.5 for different sequential measurements A, B, C, and D from experimental data

model was not possible from equivalent circuits, because three possible equivalent circuits for the clean membrane and fouled membrane were found at pH 3.0. A decrease of resistance associated to higher PVSA adsorption can be established, except for the adsorption produced at pH 4.5 where the components of equivalent circuit were found to be dependent on frequency. Additionally, our results suggest that the relaxation mechanisms at intermediate frequencies could be principally associated to polarization due to the orientation of permanent dipoles or the migration of charge carriers as result of the applied electric field.

Acknowledgments The authors thank FONDECYT (Grants No. 1070542 and 1061018) and CIPA for financial support; M. Palencia acknowledges to “Comisión Nacional de Investigación, Ciencia y Tecnología” (CONYCT-Chile) and “Centro de Investigación de Polímeros Avanzados” (CIPA-Chile) for partial financing of the Ph.D. Thesis.

References

1. Chen J, Mou H, Wang L, Matsuura T (2006) Membrane filtration. In: Wang L, Hung Y, Shammas N (eds) Advanced physicochemical treatment processes. Humana Press Inc., New Jersey, pp 203–259
2. Rivas B, Pereira E, Moreno I (2003) Water-soluble polymer–metal ion interactions. *Prog Polym Sci* 28:173–208
3. Geckeler K, Shkinev V, Spivakov Y (1988) Liquid-phase polymer-based retention (LPR)—a new method for selective ion separation. *Sep Purif Rev* 17(2):105–140
4. Rivas B, Maureira A (2008) Water-soluble polyelectrolytes containing sulfonic acid groups with metal ion binding ability by using the liquid phase polymer based retention technique. *Macromol Symp* 270:143–152
5. Cheryan M (1986) Ultrafiltration handbook. Technomic Publishing Company, Inc., Lancaster

6. Kim H, Krishnan N, Lee S, Hwang S, Kim D, Jeong K, Lee J, Cho E, Lee J, Han J, Ha H, Lim T (2006) Sulfonated poly(ether sulfone) for universal polymer electrolyte fuel cell operations. *J Power Sources* 160:353–358
7. Macdonald J (1987) Impedance spectroscopy. Emphasizing solid materials and systems. Wiley Interscience Publication, New York
8. Bisquert J (2002) Theory of the impedance of electron diffusion and recombination in a thin layer. *J Phys Chem B* 106:325–333
9. Sarac A, Ates M, Kilic B (2008) Electrochemical impedance spectroscopic study of polyaniline on platinum, glassy carbon and carbon fiber microelectrodes. *Int J Electrochem Sci* 3:777–786
10. Chilcott T, Chan M, Gaedt L, Nantawisarakul T, Fane A, Coster H (2002) Electrical impedance spectroscopy characterization of conducting membranes. I. Theory. *J Membr Sci* 195:153–167
11. Silverman D, Carrico J (1998) Electrochemical impedance technique—a practical tool for corrosion prediction. *Corrosion-NACE* 44(5):280–287
12. Barsoukov E, Ross J (2005) Impedance spectroscopy. Theory, experiment, and applications, 2nd edn. Wiley Interscience Publication, New York
13. Gaedt L, Chilcott TC, Chan M, Nantawisarakul T, Fane AG, Coster H (2002) Electrical impedance spectroscopy characterization of conducting membranes II. *J Membr Sci* 195:169–180
14. Park JS, Choi JH, Woo JJ (2006) An electrical impedance spectroscopic (EIS) study on transport characteristics of ion-exchange membrane systems. *J Colloid Interface Sci* 300:655–662
15. Kavanagh J, Hussain S, Chilcott T, Coster H (2009) Fouling of reverse osmosis membranes using electrical impedance spectroscopy: measurements and simulations. *Desalination* 236:187–193
16. Fortunato R, Branco L, Afonso C, Benavente J, Crespo J (2006) Electrical impedance spectroscopy characterization of supported ionic liquid membranes. *J Membr Sci* 270:42–49
17. Rodríguez M, Tucceri R, Florit M, Posadas DJ (2001) Constant phase element behavior in the poly(*o*-toluidine) impedance response. *Electroanal Chem* 502:82–90
18. Bordi F, Cametti C, Colby R (2004) Dielectric spectroscopy and conductivity of polyelectrolyte solutions. *J Phys Condens Matter* 16:1423
19. Chi Kao K (2004) Dielectric phenomena in solids with emphasis on physical concepts of electronic processes. Elsevier Academic Press, Amsterdam